# The Effects of Deep Cryogenic Treatment on Heat Transfer of Aluminium Heat Sink

**Rajesh Kumar MANICKAM *, Dilip Raja NARAYANA**

*Department of Mechanical Engineering, Vel Tech Rangarajan Dr. Sagunthala R&D Institute of Science and Technology, Avadi, Chennai, India*

http://doi.org/10.5755/j02.ms.37991

*Received 15 July 2024; accepted 4 November 2024*

Thermal management is critical for achieving peak performance and extending the life of electronic equipment. Heat sinks are the most effective thermal control tools. Copper and aluminium are the most used materials for heat sinks. Aluminium, in particular, attracts a lot of attention due to its lightweight and recyclability, which assures sustainability. Because of its robustness, malleability, and good thermal conductivity, the aluminium 6000 series is ideal for use in heat sink manufacturing. In this research, raw material consisting of Al6060 is turned into a square pin fin heat sink with 25 pin fins using a CNC milling machine. The natural convection heat transfer efficiency of the heat sink was identified with a specially constructed experimental setup. Four different heat inputs (15 W, 25 W, 35 W, and 45 W) were analyzed. The novelty of this work is that the heat sink undergoes deep cryogenic treatment (DCT). The soaking duration in liquid nitrogen is set at 24 hours. The heat transfer efficiency of DCT treated aluminium heat sink is compared with the bare aluminium heat sink. The testing findings revealed that when the heat input was 15W, the DCT treated square pin fin heat sink had a charging cycle that was up to 77.78 % longer than the untreated heat sink. At 25W, 35 W, and 45 W heat input, the charging cycle was 48 %, 39 %, and 28 % longer, respectively. Analyzing the discharge cycle revealed that only the 15 W heat input had an ideal discharge cycle, which was 20 % shorter than the untreated heat sink. The results are compared with the results of heat sink coupled with phase change materials (PCM) from the literature. The analysis revealed that for the DCT treated heat sink, heat input in the range of 15 W increased performance equivalent to that of PCM coupled heat sink.

*Keywords:* deep cryogenic treatment, soaking duration, natural convection, heat sink, square pin fin.

## 1. INTRODUCTION

Aluminium alloys are frequently used for constructing structural parts, power transmission units, and thermal management systems because of their higher fatigue strength, electrical conductivity, and heat dissipation efficiency [1]. Aluminium alloys have two wonderful properties: recyclability and the ability to introduce new alloying components [2]. In order to improve the performance and life cycle of components made of aluminium alloys various treatment procedures are utilized. Conventional treatment procedures used to enhance the mechanical characteristics of aluminium alloys emit pollutants. To maintain sustainability the low-cost and environmentally friendly approaches are required. The deep cryogenic treatment (DCT) is extensively rated as a sustainable treatment method and employed by researchers and industry personnel to acquire the appropriate microstructure together with the heat treatment process [3]. Cryogenic treatment which is a procedure done at an extremely low temperature can be employed to achieve enhanced qualities by causing microstructural changes [4]. DCT is considered an extra step to the regular heat treatment process [3 – 5]. Liquid nitrogen is commonly utilized as a refrigerant in DCT processes because it is generally accessible and relatively economical [6, 7].

The most essential influencing parameters for the DCT process are the holding length, homogenization temperature, and cooling temperature [5, 8]. DCT-induced lattice shrinkage severely limits the mobility of atoms and dislocations. Microstructural changes result in better mechanical properties [9]. DCT enhances the material's homogeneity by increasing precipitation density, regularity, and nucleation capacity. [10]. After DCT, some aluminium alloys show grain development and a reduction in dislocation density. The reason for this is that stored deformation energy drives grain boundary changes and variations in strain rate sensitivity in aluminium alloys at lower temperatures. [9]. The electrical conductivity of aluminium alloy is significantly high so they are highly suitable for power transmission [11, 12]. The traditional strengthening procedures used for aluminium alloys significantly diminish electrical conductivity [13 – 15]. Many study findings suggest that using the DCT technique considerably boosts the electrical conductivity and mechanical characteristics of aluminium alloys. Increasing the volume of fine precipitates enhances the electron mobility routes of metallic materials, resulting in an increase in electrical conductivity [16]. DCT can to increase dimensional stability and minimise residual stress in aluminium [17]. Abundant study is done to determine the impact of DCT on the characteristics of the 5xxx and 7xxx

* Corresponding author: M. Rajeshkumar
E-mail: *vtdl083@veltech.edu.in*

series of aluminium alloys, however, only scant research is done on the 6xxx series [18].

Systems that generate high temperatures, such as turbines, electronic components, and automobiles, require heat sinks for proper thermal management. Aluminium alloys are the most desirable option for heat sinks because of their low weight and recyclability. Significant research activities are carried out by using aluminium alloys to effectively dissipate heat. Compactness, decreased weight, low resistance, and optimal strength are all important considerations when designing a heat sink. Utilizing new design and new materials are the areas of interest for many researchers [19]. The modalities of heat transport include free convection, forced convection, and radiation. Free convection heat transmission does not require any external electricity. Fluid flow occurs in the heat sink due to uneven fluid density caused by buoyant or gravitational forces. In free convection, the majority of research activities are concentrated on the optimization of fins [20]. Heat sink research focuses primarily on eliminating flaws in internal flow, enhancing fluid turbulence, and making the heat sink temperature consistent [19]. By analyzing several heat sink designs with numerical simulation tools, it was shown that air travelling sideways is constrained, and consistent cooling in straight fins is unachievable when free convection conditions are assumed. To address this issue, numerous innovative designs, such as notched fins, inward notched fins, and many more fin designs, are proposed and tested to assure enhanced heat transfer coefficient and lower thermal resistance [21]. Cross finned heat sinks with varying fin heights displayed extremely low thermal resistance [22]. The experiments used to test the efficiency of free convection heat sinks are typically carried out using an input heating power of 80W.

By optimizing the affecting parameters, modern analytical tools and manufacturing processes may be used to develop high-performance and sustainable heat sinks [19]. In this research, aluminium alloy (Al6060) is employed, and a heat sink in the shape of a square pin fin is produced and then it is exposed to deep cryogenic treatment. An experimental setup is established, and the efficiency of DCT treated and untreated heat sinks are examined and compared.

## 2. MATERIALS AND METHODS

The In this research, an aluminium alloy (Al6060) is employed to create a heat sink. The material comes from RK Steel & Al Co (Chennai, India). The chemical composition of the samples (in weight percent) was determined using an Avio 560 max ICP optical emission spectrometer (Singapore). The testing was performed by Micro lab (an ISO/IEC 17025 material testing facility in Chennai, India). The test results are presented in Table 1. The measured figures clearly show that the chemical composition satisfies the requirements of ASTM B221 Alloy 6060. In the Vel Tech Rangarajan Dr. Sagunthala R&D Institute of Science and Technology's manufacturing lab, heat sinks are made using CNC milling. The heat sink contains 25 square pin fins, as illustrated in Fig. 1. Kavimurasu Industrial Gases (Arumbakkam, Chennai, India) distributes liquid nitrogen. The cryogenic treatment was performed in the materials lab of Vel Tech Rangarajan Dr. Sagunthala R&D Institute of Science and Technology. Fig. 2. displays a schematic of the cryogenic treatment system.

**Table 1.** Chemical analysis

| Elements, % | Symbol | Specification | Observed values |
|---|---|---|---|
| Silicon | Si | 0.30 – 0.60 | 0.457 |
| Iron | Fe | 0.10 – 0.30 | 0.230 |
| Copper | Cu | 0.10 max | 0.017 |
| Manganese | Mn | 0.10 max | 0.033 |
| Magnesium | Mg | 0.35 – 0.60 | 0.414 |
| Chromium | Cr | 0.50 max | 0.008 |
| Zinc | Zn | 0.15 max | 0.006 |
| Titanium | Ti | 0.10 max | 0.017 |
| Aluminium | Al | Remainder | 98.73 |
| Total other elements | TOE | 0.15 max | 0.024 |

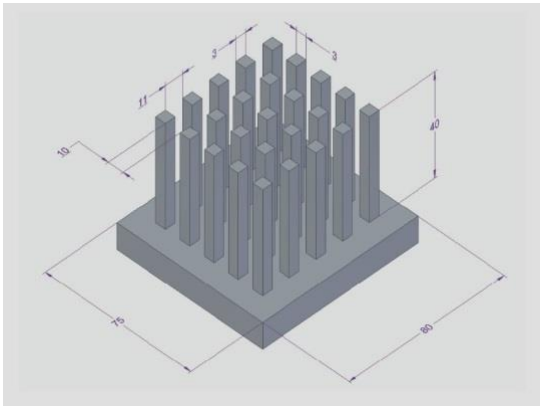

a

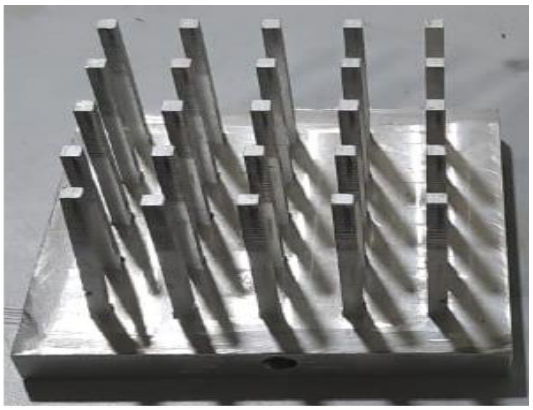

b

**Fig. 1.** a – dimensions of the heat sink; b – fabricated heat sink

The schematic depiction of the cryogenic treatment is shown in Fig. 3. The procedure begins with heating the material and then quenching it. Following quenching, the material is treated with liquid nitrogen. The time taken to treat with liquid nitrogen is referred to as soaking time. After soaking, the material will be heated again. The substance used in this research is a heat sink. The square pin fin heat sink is first homogenized in a muffle furnace at 570 degrees Celsius for an hour. The heat sink is then removed from the furnace and cooled with water to 22 degrees Celsius. The heat sink is then fully dried before immersing in liquid

nitrogen (LN2) at 196 degrees Celsius for 24 hours. After 24 hours, the heat sink is removed and returned to room temperature at a rate of 10°C/s. After reaching room temperature, the heat sink is aged for 8 hours at 190 degrees Celsius in a convection furnace [10].

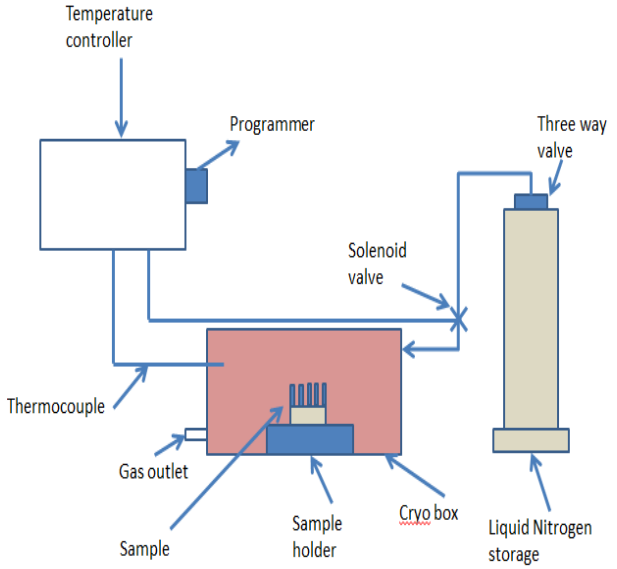


**Fig. 2.** Cryogenic treatment setup

After the deep cryogenic treatment, a slice of the heat sink is cut to 1 cm width, 1 cm height, and 1 cm thickness. To prepare for scanning electron microscopy, the heat sink's cut portion is ground on 100, 220, 400, 600, and 1200 mesh SiC papers, and then polished with 3 µm Alumina and 1 µm diamond paste. The cut piece is then etched with Keller's reagent. Immediately following metallographic preparation the microstructural investigations were conducted using a high resolution scanning electron microscope (HRSEM), Thermo scientific Apreo S from SRM University.

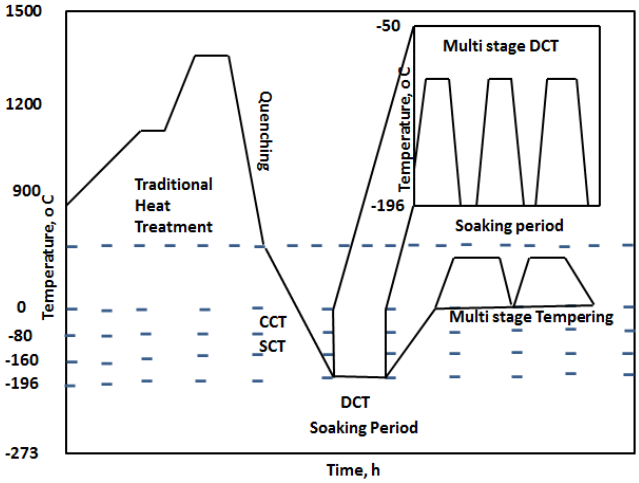


**Fig. 3.** Schematic diagram of cryogenic treatment

A custom-designed test bench was built to determine the heat dissipation capability of both the DCT-treated and untreated heat sink. A test chamber of 500 mm × 250 mm × 250 mm was built with acrylic plastics. This test chamber can decrease airflow disruptions and offer an analogous radiation background which enables the setup ideally suitable for testing natural convection conditions. Fig. 4 shows the schematic view of the experimental setup.

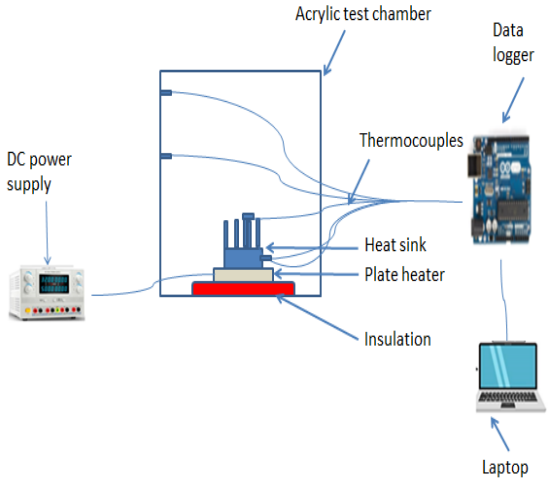


**Fig. 4.** Experimental setup

Test chamber, DC power source, plate type thermostat heater, thermocouples, and data logging system are the components available in the experimental setup. Along with this, the thermal imaging camera is also used to visibly understand the heat dissipation phenomenon of the heat sink. Arduino based data logging system was used in this experiment. Four thermocouples are kept in various places as shown in Fig. 4. Data from all the thermocouples are processed using Arduino software and the processed data can be directly loaded in Excel and graphs can be plotted. Experiments are conducted at room temperature of 33 °C.

## 3. RESULTS AND DISCUSSION

### 3.1. Microstructure

Fig. 5 a and c shows the SEM images of the untreated samples. The microstructure analysis reveals that the smaller precipitates are distributed throughout the material and the sporadic absence patches appear in the α-Al grains. The findings here are well in conformance with the findings of Matic Jovičević-Klug et al. [23]. The reason behind the formation of patches is the rapid material quenching and limited homogeneity [23]. Fig. 5 b and d shows the SEM images of DCT treated samples. Pure absence patches are not much observed in the DCT treated sample. The homogenization temperature of 570 °C [18, 27] enabled the refinement of submicron precipitates and the following Cryogenic treatment resulted in a densely formed microstructure. Comparing the untreated and DCT treated samples it is clear that the DCT resulted in a finer precipitate structure [41]. Also, it is observed that there are no significant changes in the grain boundary structure. The finer precipitates formed because of DCT can increase phonon scattering [23 – 25] but the effect will be subtle because of the fact that there are no significant changes in the precipitate distribution between the untreated and DCT treated samples.

### 3.2. Analysis of untreated heat sink

The heat sink's heating sequence is referred to as a charging cycle, and its cooling sequence as a discharging cycle [26]. The heat sink's heat transfer efficiency may be

calculated by determining how long it takes for the heat sink to achieve the junction temperature while the heat source and heat sink are in direct contact. Heat transfer efficiency is also evaluated by the time it takes for the heat sink to return to room temperature [27]. Fig. 6 a illustrates the charging and discharging cycle of an untreated heat sink. The pattern of the heating and cooling cycle varies depending on the amount of heat input. The various heat inputs used in this study are 15 W, 25 W, 35 W, and 45 W. The graphs are plotted with the start of charging time at 0 seconds.

The conclusion of the charging cycle signals the start of the draining cycle. In this study, the charging cycle finishes at 60 ºC since the junction temperature of devices that employ the natural convection mode of heat transmission ranges between 60 ºC and 80 ºC [27]. During the discharge cycle, the temperature slowly reduces and reaches the room temperature. The time taken to cool down and to reach the room temperature is usually more when compared to the charging cycle.

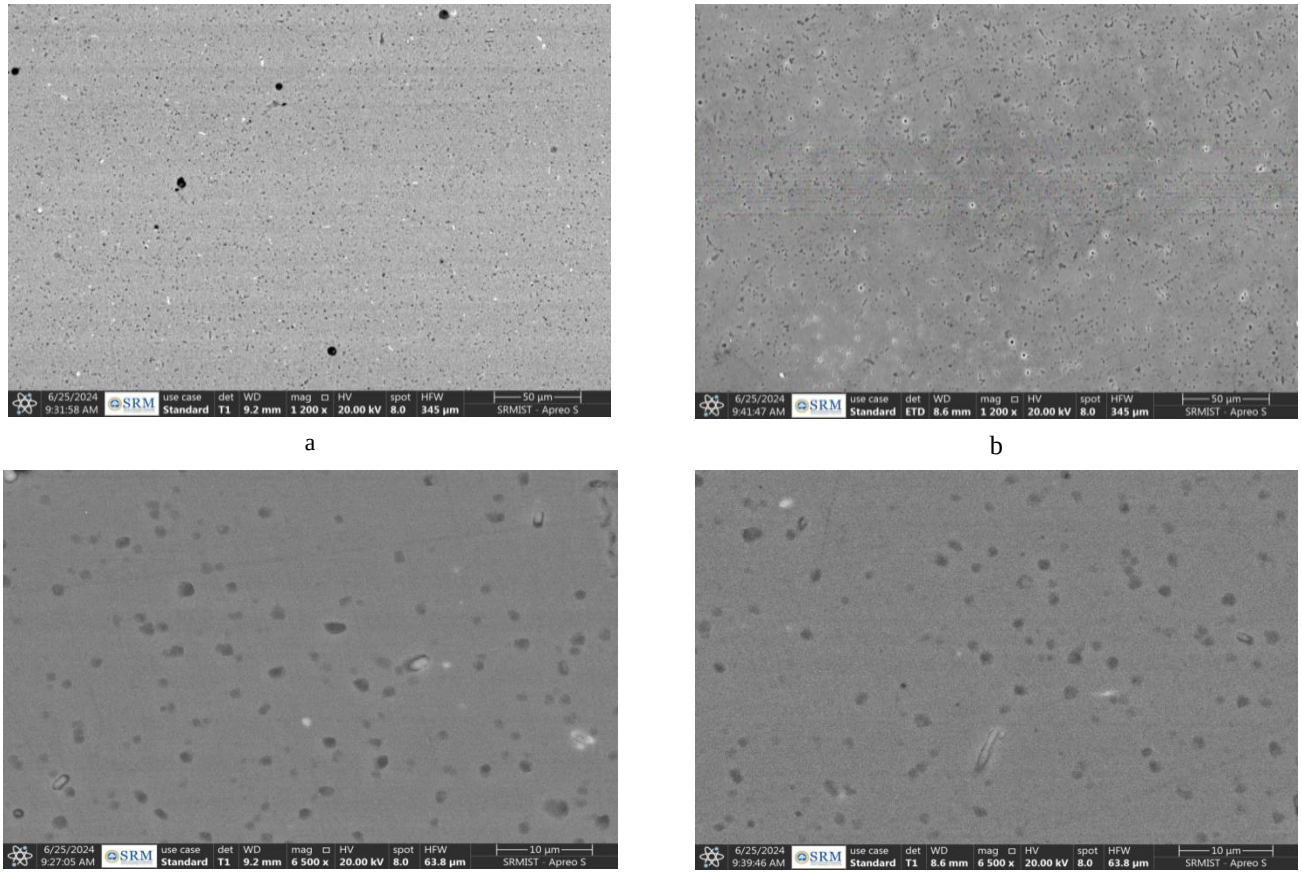

a b c d

**Fig. 5.** a – SEM image of Untreated sample at 50 µm resolution; b – SEM image of DCT sample at 50 µm; c – SEM image of untreated sample at 10 µm resolution; d – SEM image of DCT sample at 10 µm resolution

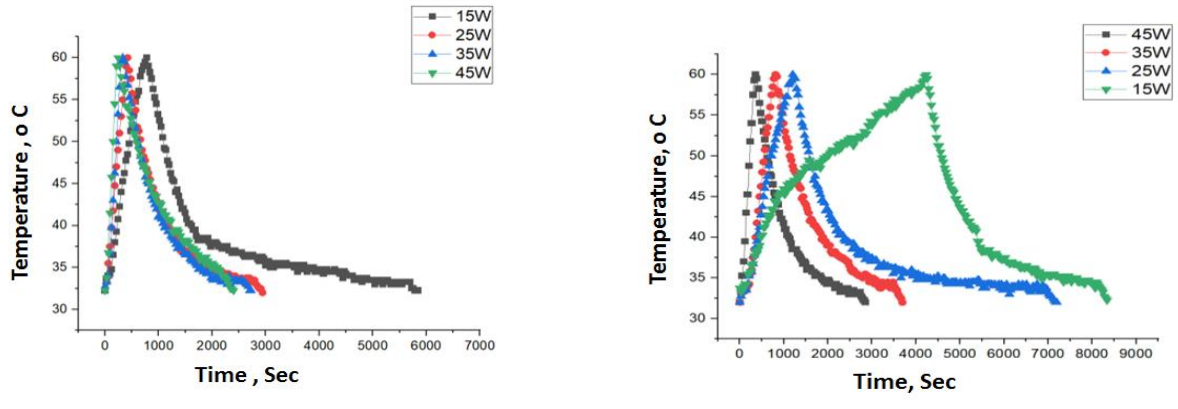


a b

**Fig. 6.** a – charging and discharging cycle of untreated heat sink; b – charging and discharging cycle of DCT treated heat sink

When the 15 W heat input is evaluated, the charging cycle lasts less than 1000 seconds, whereas the discharging cycle lasted up to 6000 seconds. The discharge cycle starts only at the end of the charging cycle [30], therefore the actual length of the discharge cycle is only 5000 seconds. The longest charging cycle and quickest discharging cycle are the ideal conditions for the optimum heat sink. The results of charging cycle of untreated heat sink and DCT treated heat sink are shown in Table 2. When tested with a 25 W heat input, the charging cycle lasted up to 600 seconds. The discharge cycle lasted up to 2400 seconds. Testing at 35 W heat input resulted in an even shorter charging cycle. It lasted fewer than 500 seconds. The discharge cycle time was less than 2300 seconds. The 45 W heat input produced the slowest charging cycle. It barely lasted up to 400 seconds. The discharge cycle lasted up to 2100 seconds. The results of discharging cycle of untreated heat sink and DCT treated heat sink are shown in Table 3.

**Table 2.** Charging cycle

| Heat input, W | Charging cycle of untreated heat sink, s | Charging cycle of DCT treated heat sink, s |
|---|---|---|
| 15 | 1000 | 4500 |
| 25 | 600 | 1250 |
| 35 | 500 | 700 |
| 45 | 400 | 500 |

**Table 3.** Discharging cycle

| Heat input, W | Discharging cycle of untreated heat sink, s | Discharging cycle of DCT treated heat sink, s |
|---|---|---|
| 15 | 5000 | 4000 |
| 25 | 2400 | 6150 |
| 35 | 2300 | 3100 |
| 45 | 2100 | 2400 |

### 3.3 Analysis of DCT treated heat sink

Fig. 6 b depicts the charging and discharging cycle of the deep cryogenic treated heat sink. At 15 W heat input, the charging cycle lasted up to 4500 seconds, which is 77.78 % longer than the untreated heat sink. The discharge cycle lasted for 4000 seconds, which is 20 % shorter than that of the untreated heat sink. At 25 W heat input, the charging cycle lasted up to 1250 seconds which is 48 % longer than the untreated heat sink. The length of the discharge cycle is 6150 seconds which is 39 % longer than the untreated heat sink. At 35 W heat input the charging cycle lasted for 700 seconds which is 28 % greater than that of the untreated heat sink. The discharging cycle lasted for 3100 seconds which is 25 % longer than that of untreated heat sink. At 45 W heat input, the charging cycle lasted for 500 seconds which is 20 % longer than the untreated heat sink. The discharging cycle lasted up to 2400 seconds which is 12. 5% longer than the untreated heat sink.

### 3.4. Thermal imaging results of the heat sink

Fig. 7 a depicts the thermal picture of an untreated heat sink. When the heat source exceeds 60 ºC at the junction, a thermal picture is captured. The blue color suggests a temperature range of 33 ºC to 40 ºC. The yellow color represents a temperature range of 45 ºC to 53 ºC. The pink color suggests a temperature range of 54 ºC to 58 ºC. The light pink color suggests a temperature range of 58 ºC to 70 ºC.

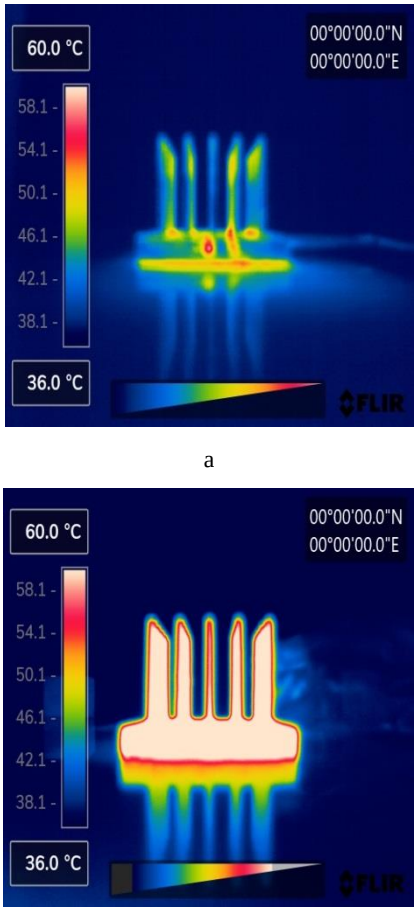


**Fig. 7.** a – thermal image of untreated heat sink; b – thermal image of DCT treated heat sink

Analyzing the thermal picture of the untreated heat sink reveals that the heat is inefficiently transmitted from the bottom to the top. The thermal picture of a DCT-treated heat sink shown in Fig. 7 b clearly demonstrates a homogeneous transfer of heat from the base to the fins. The interpretation's findings are in good agreement with those from a comparable thermal investigation on the coated heat sinks carried out by M. Arulprakasajothi [33].

### 3.5. Comparison with previous results

The findings of the researchers' use of heat sinks for thermal control are displayed in Table 4. The majority of research focuses on the use of phase-changing materials (PCM) in conjunction with nanoparticles. Not all heat dissipation happens by convection; radiation also plays a significant role in this process. Heat transmission is improved by methods to increase emissivity since metals with low emissivity, such as aluminium, are not good at it. The DCT procedure improved the total heat transmission in the current work. According to data from the PCM linked heat sink's charging and discharging cycle, the charging cycle rose by 23 % while the discharging cycle decreased by 18 % [27, 33].

**Table 4.** Comparison of results obtained from various studies on thermal management

| Source | Heat sink configuration | Dimensions, $mm^2/mm^3$ | Observation |
|---|---|---|---|
| Ali Mohammadi et al. [30] | 14 plate fins | 75×75×40 | Time to reach junction temperature increased above 15 % with the use of PCM |
| Bayat et al. [31] | 3 finned | 50×50×40 | Time to reach junction temperature increased above 10 % with the use of less nano particle in PCM |
| Joseph and Sajith [32] | 4 plate finned | 42×42×32 | Time to reach junction temperature increased above 15 % with the use of PCM |
| Tariq et al [33] | Experimental | 102×102×25 | Maximum 23 % base temperature reduction is obtained with 0.008 wt.% of RT-44HC/GNPs |
| Bondareva et al. [34] | Numerical | 30×15 | Time to reach junction temperature increased for 5 % with the use of less nanoparticles in PCM |
| Rajasekharan B et al. [29] | Rectangular box type | 90×90×50 | Time to reach junction temperature increased by15 % with the use of graphene nano particle in PCM |
| Present work | 25 Square pin fins | 75×80×40 | DCT process improved the time taken to reach junction temperature up to 22.22 % at 15 W heat input |

The obtained findings of the current study show that in the low heat input range of up to 15 W, the charging cycle may be raised up to 22.22 % and the discharge cycle can be decreased up to 20 %. Therefore, without using PCM, cryogenic treatment may be applied to affect the charging and discharging cycle time.

## 4. CONCLUSIONS

The research revealed that applying deep cryogenic treatment on an Al6060 heat sink significantly increases the charging cycle by up to 22.22 % and lowers the discharge cycle by up to 20 % when the heat input is 15 W and when there is natural convection heat transfer. For all the other heat inputs of 25 W, 35 W and 45 W the charging cycle increased by 48 %, 39 % and 28 % respectively, this is because of the improved microstructure which in turn increased the time required to reach the junction temperature. The evaluation of the discharge cycle revealed that the optimal discharge cycle was observed only for 15 W heat input. The increase in heat input negatively affects the discharge cycle. Therefore, the crucial conclusion drawn from the research is that, when heat input is within a 15 W range, applying the DCT process to the heat sink eventually improves its heat dissipation performance of the Al6060 heat sink, making it comparable to employing a heat sink in conjunction with PCM.

### REFERENCES


1. **Cam, G., Ipekoglu, G.** Recent Developments in Joining of Aluminum Alloys *International Journal of Advanced Manufacturing Technology* 91 2017: pp. 1851 – 66. https://doi.org/10.1007/s00170-016-9861-0
2. **Raabe, D., Ponge, D., Uggowitzer, P.J., Roscher, M., Paolantonio, M., Liu, C.** Making Sustainable Aluminum by Recycling Scrap: The Science of "Dirty" *Alloys Progress in Materials Science* 128 2022: pp. 100947. https://doi.org/10.1016/j.pmatsci.2022.100947
3. **Jovicevic Klug, P., Podgornik, B.** Review on the Effect of Deep Cryogenic Treatment of Metallic Materials in Automotive Applications *Metals* 10 2020: pp. 434. https://doi.org/10.3390/met10040434
4. **Das, D., Dutta, A.K., Ray, K.K.** Sub-Zero Treatments of AISI D2 Steel: Part I. Microstructure and Hardness *Materials Science and Engineering* 527 2010: pp. 2182 – 2193. https://doi.org/10.1016/j.msea.2009.10.070
5. **Gao, Q., Jiang, X.S., Sun, H.L., Fang, Y.J., Mo, D.F., Li, X.** Effect Mechanism of Cryogenic Treatment on Ferro Alloy and Nonferrous Alloy and their Weldments: A Review *Materials Today Communications* 33 2022: pp. 104830. https://doi.org/10.1016/j.mtcomm.2022.104830
6. **Akincioglu, S., Gokkaya, H., Uygur, I.** A Review of Cryogenic Treatment on Cutting Tools *International Journal of Advanced Manufacturing Technology* 78 2015: pp. 1609 – 1627. https://doi.org/10.1007/s00170-014-6755-x
7. **Padmakumar, M., Dinakaran, D.** A Review on Cryogenic Treatment of Tungsten Carbide Tool Material *Journal of Manufacturing and Materials Processing* 36 2021: pp. 637 – 59. https://doi.org/10.1080/10426914.2020.1843668
8. **Razavykia, A., Delprete, C., Baldissera, P.** Correlation Between Microstructural Alteration, Mechanical Properties and Manufacturability after Cryogenic Treatment: A Review *Materials* 12 2019: pp. 3302. https://doi.org/10.3390/ma12203302
9. **Enze Yao, A., Huijie Zhang, A., Kang Ma, B., Conggang, Ai,B., Qiuzhi Gao, A., Xiaoping Lin, A.** Effect of Deep Cryogenic Treatment on Microstructures and Performances of Aluminum Alloys: A Review *Journal of Materials Research and Technology* 26 2023: pp. 3661 – 3675. https://doi.org/10.1016/j.jmrt.2023.08.140
10. **Matic, K., Levi, T., Patricia, K., Goran, D., Laszl Almasy, F., Bryan, L., Julie, M., Cairney Bojan, P.** Multiscale Modification of Aluminum Alloys with Deep Cryogenic Treatment for Advanced Properties *Journal of Materials Research and Technology* 26 2022: pp. 3062 – 3073. https://doi.org/10.1016/j.jmrt.2022.10.089
11. **Karabay, S., Feyzullahoglu, E.** Determination of Early Failure Sources and Mechanisms for Al 99.7% and Al-Mg-Si Alloy Bare Conductors Used in Aerial Transmission Lines *Engineering Failure Analysis* 38 2014: pp. 1 – 15. https://doi.org/10.1016/j.engfailanal.2013.12.002
12. **Wang, Y., Zhu, L.J., Niu, G.D., Mao, J.** Conductive Al Alloys: The Contradiction between Strength and Electrical Conductivity *Advanced Engineering Materials* 23 2021: pp. 1e22.

https://doi.org/10.1002/adem.202001249

13. **Lei, G.P., Wang, B., Lu, J., Wang, C., Li, Y.M., Luo, F.H.** Effects of Solid Solution Temperature on the Microstructure and Properties of 6013 Aluminum Alloy *Materials Chemistry and Physics* 280 2022: pp. 125829. https://doi.org/10.1016/j.matchemphys.2022.125829
14. **Wang, Y.C., Liu, M.W., Xiao, W.L., Zhao, W.T., Ma, C.L.** Effects of Multi-Stage Aging Treatments on the Precipitation Behavior and Properties of 7136 Aluminum Alloy *Journal of Alloys and Compounds* 814 2020: pp. 152256. https://doi.org/10.1016/j.jallcom.2019.152256
15. **Khangholi, S.N., Javidani, M., Maltais, A., Chen, X.G.** Investigation on Electrical Conductivity and Hardness of 6xxx Aluminum Conductor Alloys with Different Si levels *In: Proceedings of the 17th international conference on Aluminium Alloys Electrical Network* (26 – 29) 2020: pp. 08002. https://doi.org/10.1051/matecconf/202032608002
16. **Cai, S.L., Li, D.Q., Liu, S.C., Si, J.J., Gu, J., Zhou, L.X.** Cryogenic Reciprocating Torsion Induced Nanoscale Precipitation in Aluminum Wire with Exceptional Strength and Electrical Conductivity *Materials Science and Engineering* 860 2022: pp. 144276. https://doi.org/10.1016/j.msea.2022.144276
17. **Zhou, C.A., Sun, Q.D., Qian, D.Q., Liu, J.W., Sun, J., Sun, Z.L.** Effect of Deep Cryogenic Treatment on Mechanical Properties and Residual Stress of AlSi10Mg Alloy Fabricated by Laser Powder Bed Fusion *Journal of Materials Processing and Technology* 303 2022: pp. 117543. https://doi.org/10.1016/j.jmatprotec.2022.117543
18. **Gao, W., Wang, X., Chen, J., Ban, C., Cui, J., Lu, Z.** Influence of Deep Cryogenic Treatment on Microstructure and Properties of 7A99 Ultra-High Strength Aluminum Alloy *Metals* 9 2019: pp. 631. https://doi.org/10.3390/met9060631
19. **Jingnan, L., Li, Y.** Recent Development of Heat Sink and Related Design Methods *Energies* 16 2023: pp. 7133. https://doi.org/10.3390/en16207133
20. **Zhang, K., Liu, H., Du, F., Chen, X., Li, B., Hong, J.** MMC-based Heat Sink Topology Optimization Design for Natural Convection Problems *International Journal of Thermal Sciences.* 192 2023: pp. 108376. https://doi.org/10.1016/j.ijthermalsci.2023.108376
21. **Muneeshwaran, M., Tsai, M.K., Wang, C.C.** Heat Transfer Augmentation of Natural Convection Heat Sink through Notched Fin Design *Inernational Communications in Heat and Mass Transfer* 142 2023: pp. 106676. https://doi.org/10.1016/j.icheatmasstransfer.2023.106676
22. **Feng, S., Shi, M., Yan, H., Sun, S., Li, F., Lu, T.J.** Natural Convection in a Cross-Fin Heat Sink *Applied Thermal Engineering* 132 2018: pp. 30 – 37. https://doi.org/10.1016/j.applthermaleng.2017.12.049
23. **Matic, J., Rok, R., Patricia, J., Bojan, P.** Influence of Deep Cryogenic Treatment on Natural and Artificial Aging of Al-Mg-Si Alloy EN AW 6026 *Journal of Alloys and Compounds* 899 2022: pp. 163323. https://doi.org/10.1016/j.jallcom.2021.163323
24. **Araghchi, M., Mansouri, H., Vafaei, R., Guo, Y.** A Novel Cryogenic Treatment for Reduction of Residual Stresses in 2024 Aluminum Alloy *Materials Science and Engineering* 689 2017: pp. 48 – 52. https://doi.org/10.1016/J.MSEA.2017.01.095
25. **Kenyon, M., Robson, J., Fellowes, J., Liang, Z.** Effect of Dispersoids on the Microstructure Evolution in Al – Mg – Si Alloys *Advanced Engineering Materials* 21 2019: pp. 1800494. https://doi.org/10.1002/adem.201800494
26. **Rajesh, A., Athul, G., Srikanth, R., Balaji, C.** Experimental and Numerical Studies on Heat Transfer from a PCM based Heat Sink with Baffles *International Journal of Thermal Sciences* 159 2020: pp. 106525. https://doi.org/10.1016/j.ijthermalsci.2020.10652
27. **Rajasekaran, B., Kumaresan, G., Arulprakasajothi, M., Beemkumar, N.** Exploring Thermal Response in Aluminium Heat Sinks with Variable Surface Roughness for Enhanced Cooling *Journal of Thermal Science* 28 2024: pp. 2513 – 2525. https://doi.org/10.2298/TSCI230916013B
28. **Alimohammadi, M., Aghli, Y., Alavi, E.S., Sardarabadi, M., Passandideh, M.** Experimental Investigation of the Effects of Using Nano/Phase Change Materials (NPCM) as Coolant of Electronic Chipsets, Under Free and Forced Convection *Applied Thermal Engineering* 111 2017: pp. 271 – 279. https://doi.org/10.1016/j.applthermaleng.2016.09.028
29. **Bayat, M., Faridzadeh, M.R., Toghraie, D.** Investigation of Finned Heat Sink Performance with Nano Enhanced Phase Change Material (NePCM) *Thermal Science and Engineering Progress* 5 2018: pp. 50 – 59. https://doi.org/10.1016/j.tsep.2017.10.021
30. **Joseph, M., Sajith, V.** Graphene Enhanced Paraffin Nano Composite based Hybrid Cooling System for Thermal Management of Electronics *Applied Thermal Engineering* 163 2019: pp. 114342. https://doi.org/10.1016/j.applthermaleng.2019.114342
31. **Tariq, S.L., Ali, H.M., Akram, M.A., Janjua, M.** Experimental Investigation on Graphene based Nanoparticles Enhanced Phase Change Materials (GbNePCMs) for Thermal Management of Electronic Equipment *Journal of Energy Storage* 30 2020: pp. 101497. https://doi.org/10.1016/j.est.2020.101497
32. **Bondareva, N.S., Gibanov, N.S., Sheremet, M.A.** Computational Study of Heat Transfer Inside Different PCMs Enhanced by Al2O3 Nanoparticles in a Copper Heat Sink at High Heat Loads *Nanomaterials* 10 2020: pp. 284. https://doi.org/10.3390/ nano10020284
33. **Arulprakasajothi, M., Dilip Raja, N., Saranya, A., Elangovan, K., Murugapoopathi, S., Poyyamozhi, N., Kassain, T., Amesha, T.** Optimizing Heat Transfer Efficiency in Electronic Component Cooling through Fruit Waste Derived Phase Change Material *Journal of Energy Storage* 80 2024: pp. 110238. https://doi.org/10.1016/ j.est.2023.110238